

## Experimental and modelling studies of hydrogen generation from NaBH<sub>4</sub>/Al<sub>2</sub>O<sub>3</sub> nanoparticles/H<sub>2</sub>O system with CoCl<sub>2</sub> as a catalyst

A. Sudan, A. Kaur\*, D. Gangacharyulu, R. K. Gupta

*Department of Chemical Engineering, Thapar Institute of Engineering and Technology, Patiala, India*

Received: August 24, 2020; Revised: December 13, 2020

Sodium borohydride is extensively used for solid-state hydrogen storage & generation and considered as the most prominent chemical hydride due to its high hydrogen storage capacities. In relation to the previous studies on NaBH<sub>4</sub>/Al<sub>2</sub>O<sub>3</sub> nanoparticles/H<sub>2</sub>O system with CoCl<sub>2</sub> as a catalyst which presented rate kinetics, this study exclusively deals with the adsorption kinetics in this system. The study includes a series of equations using Langmuir-Hinshelwood adsorption model that represents adsorption phenomenon occurring in the solution in correspondence with the equations from the literature. These equations remarkably lead through in obtaining the surface coverage parameter presenting the adsorption of borohydride ions on catalyst surface. Furthermore, effect of temperature is observed on the concentration of NaBH<sub>4</sub> to obtain experimental hydrogen generation. This parameter calculates [C] that is final concentration against each initial concentration of NaBH<sub>4</sub>, amount of adsorbed species ( $q_e$ ) on catalyst surface, Langmuir-Hinshelwood adsorption constants, surface coverage ( $\theta_A$ ) and enthalpy of the system. Role of chemical behaviour of alumina nanoparticles is also elaborated in this study, which promotes the overall hydrogen generation in combination of rise in temperature.

**Keywords:** Adsorption, Langmuir-Hinshelwood, Nanoparticles, Enthalpy, Hydrogen generation.

### INTRODUCTION

The growing concern about depleting oil reserves and harmful effects of carbon dioxide gas emissions in atmosphere are key factors that encourage the development of new and renewable energy technologies [1]. Hydrogen, the zero carbon fuel, is a resolution considered worldwide for a secure energy future so as to lessen the effect of CO<sub>2</sub> in air [2]. However, many crucial and technical challenges remain to be addressed before hydrogen-based energy can become extensively accessible and economical [3, 4]. Additionally, on-board hydrogen storage has been identified as one of the technical difficulties in the implementation of hydrogen economy on global scale [5, 6]. Technologies for hydrogen storage should be considerably advanced in a hydrogen-based energy system; particularly in the transportation sector [5, 7-9]. Storing hydrogen is relatively difficult because of its low density and critical temperature. There are three ways to store hydrogen: (a) compressed gas, (b) cryogenic liquid hydrogen (LH<sub>2</sub>) and (c) solid-state hydrogen storage [10]. The main disadvantage of compressed gas and cryogenic liquid hydrogen storage is that hydrogen can only be stored in pressurized form (up to 700 bar) or cryo-compressed form (down to -253°C).

Additionally, various safety concerns and sophisticated technologies are also required to adopt this mode of hydrogen storage.

Many novel concepts of hydrogen storage had emerged in past decades like chemical hydrogen storage or material-based hydrogen storage. One of them is solid-state hydrogen storage that involves storage of hydrogen in complex chemical hydrides. These hydrides have high hydrogen content and hydrogen can be released from them through several chemical pathways like hydrolysis and thermolysis [11-14]. Hydrolysis of chemical hydrides takes place at comparatively moderate temperatures and gives more promising theoretical hydrogen storage efficiencies than thermolysis [15].

Among all chemical hydrides, sodium borohydride (NaBH<sub>4</sub>) has been considered as the most attractive hydrogen storage material, as it provides a safe and practical mean of storing hydrogen and has high hydrogen content. It undergoes hydrolysis reaction like other hydrides and forms the byproduct sodium metaborate (NaBO<sub>2</sub>). By dissolving sodium borohydride in a basic solution, a highly stable aqueous solution is formed and further hydrogen release could be initiated with an active catalyst during NaBH<sub>4</sub> hydrolysis reaction.

\* To whom all correspondence should be sent:  
E-mail: er.arsh87@gmail.com

Moreover, reaction stoichiometry states that 1 g of NaBH<sub>4</sub> solution will produce 2.4 L of hydrogen at normal temperature and pressure (STP). On this basis, it gives gravimetric storage capacity of 10.8 wt%. Furthermore, storing hydrogen in the form of aqueous solutions has many advantages. It is worth mentioning that hydrogen with NaBH<sub>4</sub> could be released at ambient conditions, thus increasing its application for portable fuel cells [16-18]. There is a remarkable progress in manufacturing of proton exchange fuel cells to be used in NaBH<sub>4</sub> hydrogen generation systems [19]. Also, there is a significant progress in compact hydrogen storage that would meet higher hydrogen yields per unit mass and volume and is efficient enough to work at low temperature [20].

A significant research towards synthesizing an active catalyst is a step forward for development of NaBH<sub>4</sub>-based on-board hydrogen generation (HG) systems [21]. Cobalt(II) chloride, nickel(II) chloride, iron(II) chloride, copper(II) chloride and manganese(II) chloride are non-noble catalysts that are investigated with time for NaBH<sub>4</sub> hydrolysis. Besides this, noble metal catalysts like ruthenium and platinum with different supporting materials as platinum loaded on LiCoO<sub>2</sub> or ruthenium loaded on TiO<sub>2</sub> are also studied. Due to cost factors, it is not feasible to make use of noble metal catalysts for widespread applications in hydrogen storage systems. Out of all above, cobalt(II) chloride is found to be highly active for NaBH<sub>4</sub> hydrolysis reaction [21-23].

Various kinetic models are studied with respect to the NaBH<sub>4</sub>-based hydrolysis system like zero order, first order, second order, power law model, Langmuir-Hinshelwood model and Michaelis and Menton models [6]. Zero order kinetic model is based on the linear behaviour of hydrogen generation volume with fixed concentrations of NaBH<sub>4</sub>, NaOH and catalyst. Zero order kinetic model is not reliable because usually zero order kinetics shifts from zero order to non-zero order with respect to NaBH<sub>4</sub> concentrations due to by-product formation and increase in water consumption [5].

Also, first order and second order kinetic models give the dependence on catalyst and NaBH<sub>4</sub> concentrations and are unable to relate hydrogen generation rate (HGR) with NaOH. Michaelis and Menton model is based on constant NaOH and temperature consideration thus limiting its practical use. On the other hand, power law kinetic model is based on the concentration of catalyst, NaBH<sub>4</sub> and NaOH. This model could predict order with respect to each factor independently. It does not require any

assumption, hence making it useful for practical applications [6].

Therefore, the authors have used the power law kinetic model in previous studies to understand the kinetics of NaBH<sub>4</sub>/H<sub>2</sub>O system with CoCl<sub>2</sub> as catalyst and alumina nanoparticles (20 nm) as promoter. Previous research revealed an incredible high efficiency of 99.34% at a mass ratio of 0.09: 0.7 for Al<sub>2</sub>O<sub>3</sub>: NaBH<sub>4</sub> with theoretical hydrogen density of 10.76 wt% and experimental hydrogen density of 10.69 wt%. This value is high enough to ensure the overall conversion of NaBH<sub>4</sub> in terms of hydrogen release in the system [25].

As the previous published studies were specifically based on rate kinetics, the new insight of this research is to observe the adsorption kinetics of NaBH<sub>4</sub>/Al<sub>2</sub>O<sub>3</sub> nanoparticles/H<sub>2</sub>O system with CoCl<sub>2</sub> as a catalyst. Consequently, Langmuir-Hinshelwood (L-H) model is reasonably used to develop novel equations for this system representing the surface coverage of sodium borohydride ions on the catalyst in the solution. Experimentation studies are conducted to observe variation in concentration of NaBH<sub>4</sub> with time at different temperatures and previous studies lacked these measurements. Finally, the observed data are used to calculate the surface coverage of borohydride ions on catalyst surface.

## EXPERIMENTAL

The reaction occurs in a three-port 250 mL reactor and reagents NaBH<sub>4</sub>, Al<sub>2</sub>O<sub>3</sub> and CoCl<sub>2</sub> are primarily added together in solid form in the reactor before the reaction starts. Then, aqueous solution of NaOH (10 mL) is added by a pressure equalizing funnel connected to the reactor from the central port. Predetermined amounts of reactants are used for the reaction like NaBH<sub>4</sub> (1, 1.25, 1.50, 1.75 moles/L), CoCl<sub>2</sub> (0.02 moles/L), Al<sub>2</sub>O<sub>3</sub> (0.09 moles/L) and NaOH (1.4 mole/L). The concentration of Al<sub>2</sub>O<sub>3</sub>, CoCl<sub>2</sub> and NaOH is considered on the basis of preliminary experiments conducted to observe the maximum hydrogen rate in previous studies [24, 25]. Left-hand port is used to attach the thermometer to monitor the change in reaction temperature. Evolved hydrogen gas is observed as soon as the aqueous NaOH solution from the central port comes in contact with the reagents (NaBH<sub>4</sub>, Al<sub>2</sub>O<sub>3</sub> and CoCl<sub>2</sub>) already present in solid form in the reactor. There is continuous stirring action observed by the evolved hydrogen gas bubbles which could lead to homogeneous dispersion of the catalyst in the solution. However, the right-hand port is attached to the cylindrical pipe that guides the generated hydrogen to the inverted cylinder (3L capacity) that

is a part of the water replacement system consisting of a container (4L capacity). The experiments are performed at four different temperatures that are 293, 303, 313 and 323K, thus, a heating mantle is used to control these temperatures whereas, to prevent the fluctuation of temperature during the reaction a water bath is used taking in consideration a variation of  $\pm 0.2^\circ\text{C}$ .

The figure of experimental setup is similar to the setup used in previous works [24, 25] thus, it is provided in the supplementary section.

#### *Application of Langmuir-Hinshelwood kinetic model*

For the present system, Langmuir-Hinshelwood (L-H) model states the adsorption of adsorbate species (BH<sup>+</sup>) on the catalyst surface as the reaction in liquid phase [27]:



Here, BH<sub>4</sub><sup>-</sup> are borohydride ions and (\*) presents the catalytic surface in the solution. It is assumed that for a heterogeneous catalytic reaction, adsorption of reactant molecule occurs on the catalyst surface. Consequently, there is a possibility of formation of a strong chemical bond on the catalyst surface by the phenomenon called as chemisorption. However, few adsorbate and adsorbant combinations are formed because chemisorption involves single layer adsorption of reactant on catalyst surface. Therefore, this heterogeneous catalyst system would depend on the concentration of chemisorbed molecules. Accordingly, the concentration of reactants is related with their respective solid surface coverage on the catalyst [28, 29].

There are series of steps that occur during the hydrolysis reaction of sodium borohydride which would relate to the above theory. Firstly, for simplification, it is supposed that all reactants are in the same phase (liquid), all adsorption sites have similar energies of adsorption and there is no interaction among adsorbed species.

a) The change in concentration of sodium borohydride [C] with time is calculated by equation 2:

$$[C] = C_{A0} \left(1 - \frac{V_{\text{H}_2}}{V_{\text{H}_2\text{max}}}\right) \quad (2)$$

where, C<sub>A0</sub> is the initial concentration of NaBH<sub>4</sub> in moles/L. V<sub>H<sub>2</sub></sub> is the experimental value of hydrogen generated at each time point and V<sub>H<sub>2</sub>max</sub> is the maximum amount of hydrogen that can be generated by the system in litres [27].

b) The maximum amount of hydrogen generated is calculated as follows:

$$V_{\text{H}_2\text{max}} = \frac{\text{amount of NaBH}_4 \text{ taken}}{\text{molecular weight of NaBH}_4} \times 4 \times \frac{22.4}{273} \times T \quad (3)$$

where, T = reaction temperature in K, constant (4) is the number of molecules of hydrogen generated by stoichiometry given by equation:



c) further, (q<sub>e</sub>) is the concentration of adsorbed species calculated by:

$$q_e = \frac{C_A - C_{A0}}{C_{\text{catalyst}}} \times \text{Volume of the solution (L)} \quad (5)$$

## RESULTS AND DISCUSSION

Previous studies presented the role of each individual reagent that promoted hydrogen generation rate. NaBH<sub>4</sub> is the prime component during the reaction and supplier of borohydride ions in the solution.

CoCl<sub>2</sub> is a catalyst precursor; it is reduced by borohydride ions to form catalytically active Co<sub>2</sub>B species in the solution [38].

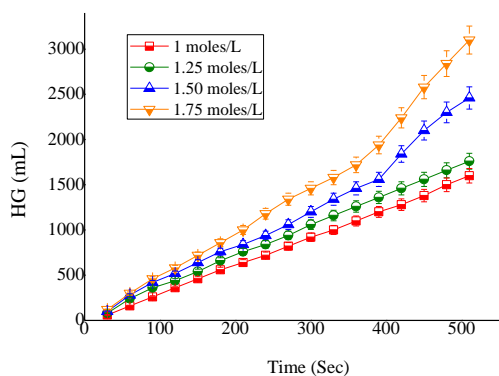
Alumina acts as a catalyst promoter which provides a synergistic catalytic effect because of the formation of Co<sub>2</sub>B species and hydroxylates of alumina. This results in the formation of Co/Al complexes like cobalt aluminates which further promote the activity of Co<sub>2</sub>B active species resulting in intensifying NaBH<sub>4</sub> hydrolysis in the solution [32, 33]. These interpretations are backed by physiochemical methods like XRD and FTIR characterization analysis used to study the residue left after the completion of the reaction. The results undoubtedly present that cationic adsorption of Co<sup>+2</sup> or Na<sup>+</sup> occurs on the hydroxide layer of alumina surface that leads to the formation of cobalt and sodium aluminates in the solution (Figures S2 & S3).

Lastly, NaOH helps in preventing passivation of alumina surface which helps alumina to form Co/Al and Co/Na complexes and ultimately promotes hydrolysis of NaBH<sub>4</sub> [24, 25].

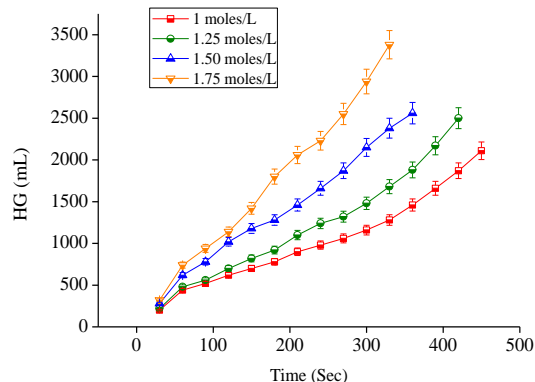
In the present study hydrogen generation is observed at increasing temperatures (293, 303, 313 and 323 K) at different concentrations of NaBH<sub>4</sub> (Figures 1, 2, 3 and 4) with respect to time [30-32]. The figures significantly confer the increasing trend of hydrogen generation (HG) with temperature whereas in previous studies, the trend of increase in HG with respect to NaBH<sub>4</sub> was observed only at room temperature. Additionally, these plots of HG with time also provide the experimental hydrogen generation at each concentration and varying set of temperatures. This experimental hydrogen obtained plays a vital role in observing the adsorption kinetics and ultimately calculating the surface coverage of

borohydride ions on the catalyst surface in this system. The generated experimental hydrogen is used in equation 2 formulated with V<sub>max</sub> (equation 3) to calculate the final concentration of NaBH<sub>4</sub> (Table 1). Further, the concentration of adsorbed species

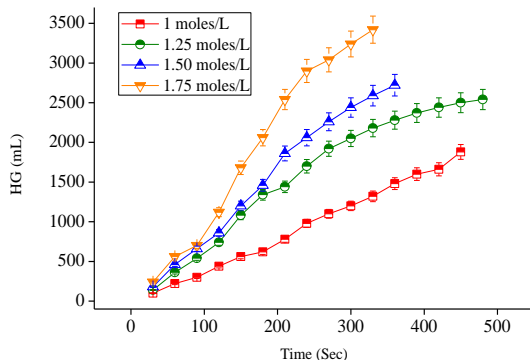
(q<sub>e</sub>) is calculated by using equation 5. This finally provides the values of surface coverage of borohydride ions on the catalyst (Table 2) at varying temperatures.



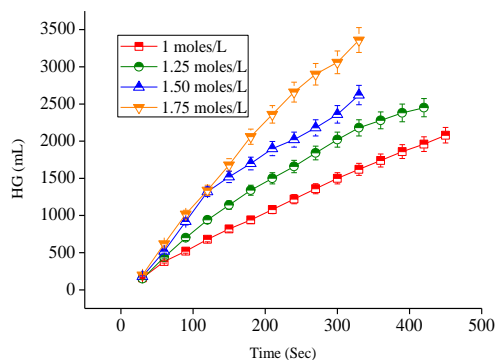
(1) At 293K



(2) At 303K



(3) At 313K



(4) At 323K

Figures 1, 2, 3 & 4. Plots of hydrogen generation with respect to time at various temperatures.

Table 1. Final concentration of NaBH<sub>4</sub> at different temperatures

| S. No. | Initial concentration     | Final concentration at various temperatures (moles/L) |          |          |          |
|--------|---------------------------|---|----------|----------|----------|
|        | C <sub>A0</sub> (moles/L) | [C] 293K  | [C] 303K | [C] 313K | [C] 323K |
| 1.     | 1                         | 0.02  | 0.03     | 0.04     | 0.09     |
| 2.     | 1.25                      | 0.05  | 0.06     | 0.07     | 0.08     |
| 3.     | 1.50                      | 0.09  | 0.18     | 0.21     | 0.22     |
| 4.     | 1.75                      | 0.12  | 0.13     | 0.16     | 0.27     |

Table 2. Values of q<sub>e</sub> and θ<sub>A</sub> at 293 and 323K

| Sample No. | C <sub>A0</sub> (moles/L) | [C] (moles/L) at 293K | [C] (moles/L) at 323K | q <sub>e</sub> (moles/g) at 293K | q <sub>e</sub> (moles/g) at 323K | θ <sub>A</sub> at 293K | θ <sub>A</sub> at 323K |
|------------|---------------------------|-----------------------|-----------------------|----------------------------------|----------------------------------|------------------------|------------------------|
| 1.         | 1                         | 0.016                 | 0.019                 | 0.20                             | 0.20                             | 0.4                    | 0.6                    |
| 2.         | 1.25                      | 0.05                  | 0.073                 | 0.23                             | 0.24                             | 0.5                    | 0.8                    |
| 3.         | 1.50                      | 0.09                  | 0.22                  | 0.28                             | 0.26                             | 0.60                   | 0.9                    |
| 4.         | 1.75                      | 0.12                  | 0.27                  | 0.29                             | 0.3                              | 0.8                    | 1                      |

Table 1 gives information of the final concentration of NaBH<sub>4</sub> at various temperatures (293, 303, 313 and 323K) and the mathematical calculations confirm that the final concentration of NaBH<sub>4</sub> in solution increases with an increase in temperature [36, 37].

Table 2 provides the values of q<sub>e</sub> (amount of absorbed species) and θ<sub>A</sub> (surface coverage). Here, an increasing trend in the values is observed with respect to temperature and NaBH<sub>4</sub> concentration.

Consequently, Langmuir adsorption isotherm constants (k<sub>1</sub>, k<sub>2</sub>, k<sub>3</sub> and k<sub>4</sub>) at 293, 303, 313 and 323K and enthalpy of this system are calculated by Van't Hoff equation 6:

$$\frac{d}{dt} \ln(K_{eq}) = \frac{\Delta H}{RT^2} \quad (6)$$

Here, ln(K<sub>eq</sub>) signifies the change in equilibrium constant with change in temperature. Thus, by plotting ln(K<sub>eq</sub>) and 1/T (Figure 5) the enthalpy of the system is calculated as -47 kJ/mole.

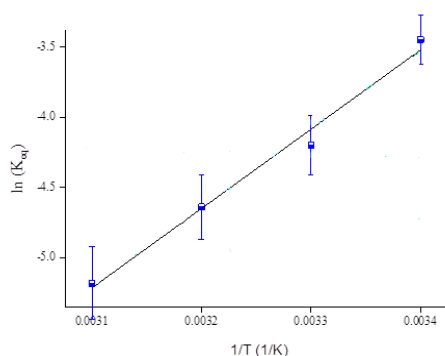


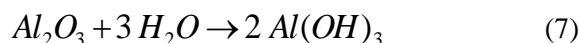
Figure 5. Plot of 1/[T] and ln(Keq)

When these results are interrelated with previous interpretations it is understood that temperature is dominantly promoting the role of alumina as a catalyst promoter in the solution and ultimately causing an increase in surface coverage of borohydride species on the catalyst surface. Therefore, the present study would also comprehensively describe the chemical behavior of alumina in the solution to provide a clear vision on how temperature is promoting adsorption kinetics in the solution.

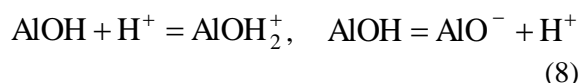
Chemical properties of alumina are elaborated as given below which in combination with rise in temperature have a considerable effect on hydrogen generation.

(a) Hydrophilic nature of alumina. Due to the chemical behaviour of γ-Al<sub>2</sub>O<sub>3</sub> in the solution at least a monolayer of water is chemisorbed by alumina. When the surface is hydrated, water molecules are

chemisorbed on the top oxide layer of γ-Al<sub>2</sub>O<sub>3</sub> as shown in reaction 7 [33]:



(b) Amphoteric nature of alumina. Reactive functional groups (hydroxyl ions) are coordinated in various ways to aluminum cations on the alumina surface like hydroxyl group with one aluminum ion and hydroxyl groups with two aluminum ions. Basic nature of alumina is given by singly coordinated hydroxyl groups and acidic nature by hydroxyl ions coordinated with two aluminum ions. The ionization reactions presenting the acidic and basic nature of alumina are given in [34]:



The hydroxyl groups in the present system are expected to be singly co-ordinated with aluminum ions thus, developing a basic nature in the solution.

(c) Iso-electric point and pH of the solution. This is explained by the principle of electro-neutrality, as in acidic medium the oxide particle will be positively charged and to compensate this charge a layer of particles with opposite charge (negative charge) will be present in the solution that will surround the oxide particles. Similarly, in basic medium, oxide particles will be negatively charged and a layer of positively charged particles will be present in the solution that surrounds the oxide particle. Furthermore, the iso-electric point is the value of solution pH when the net oxide particle charge is zero. The iso-electric point of alumina is at pH = 8, which implies that alumina will adsorb anions at a solution pH lower than 8 and adsorb cations at a solution pH higher than 8 [34, 35]. The present system is at pH = 9, therefore, adsorption of Co<sup>+2</sup> and Na<sup>+2</sup> cations occurs on alumina surface.

Thus, hydrophilic nature, amphoteric nature, iso-electric point and pH of solution are a few chemical behavioral characteristics of alumina that promote its reactivity as a catalyst promoter in the solution.

Therefore, it is interpreted that increase in temperature speeds up the formation of alumina reactivity and formation of cobalt and sodium aluminates in the solution and results in rise in affinity, as well as diffusion capacity of borohydride ions towards the catalyst resulting in high surface coverage of borohydride ions on the catalyst surface with rise in temperature [36, 37].

## CONCLUSIONS

The present research is an exclusive study on the adsorption properties of the NaBH<sub>4</sub>/γ-Al<sub>2</sub>O<sub>3</sub> nanoparticles/ H<sub>2</sub>O system with CoCl<sub>2</sub> as a catalyst. Langmuir-Hinshelwood adsorption model is extensively used predicting the equations in correspondence with the present hydrogen generation system. The effect of increasing temperature is examined at varying concentration of NaBH<sub>4</sub> and thus experimental hydrogen generation is monitored. This ultimately leads to calculate parameters like final NaBH<sub>4</sub> concentration, q<sub>e</sub> that is concentration of the adsorbed species, Langmuir adsorption isotherms constants and surface coverage (θ<sub>A</sub>). It is observed that all these parameters increase with increase in temperature. Furthermore, Van't Hoff equation calculates the value of enthalpy of this system to be -47 kJ/mole. Mathematical calculations describe the increase in surface coverage of borohydride ions with temperature. This result is also supported by the chemical properties of alumina like hydrophilic nature, amphoteric nature, isoelectric point and pH of the solution as they enhance the rate of hydrogen generation in the system. The study overall describes novel mathematical observations and adsorption studies of the NaBH<sub>4</sub>/γ-Al<sub>2</sub>O<sub>3</sub> nanoparticles/ H<sub>2</sub>O system with CoCl<sub>2</sub> which directly contributes to the use of NaBH<sub>4</sub> for practical fuel cell applications.

**Acknowledgements:** The authors gratefully acknowledge the support provided by the management of Thapar Institute of Engineering and Technology, Patiala for providing the necessary facilities to carry out this research work and guidance provided by Prof. Pramod K. Bajpai (Ex. Distinguished Professor, Thapar University, India) and Dr. Chitrakshi Goel (Research Officer, Swansea University, Swansea, Wales, U.K.)

## REFERENCES

1. S. Kaufman, *J. Chemical Society*, **64**, 307 (1985).
2. H. I. Schlesinger, H. C. Brown, A. E. Finholt, J. R. Gilbreath, H. R. Hoekstra, E. K. Hyde, *J. American Chem. Society*, **75**, 215 (1953).
3. K. Cowey, K. J. Green, G. O. Mepsted, R. Reeve, *Current Opinion in Solid State and Material Science*, **8**, 367 (2004).
4. J. S. Zhang, D. Hazra, T. S. Fisher, P. V. *J. Power Sources*, **32**, 2298 (2006).
5. S. C. Amendola, G. S. L. Sharp, J. M. Saleem, M. T. Kelly, P. J. Petillo, M. Binder, *J. Power Sources*, **85**, 186 (2000).
6. R. Retnamma, A. Novais, C. M. Rangel, *Int. J. Hydrogen Energy*, **22**, 1649 (2011).
7. Y. Shang, R. Chen, *Energy and Fuels*, **20**, 2149 (2006).
8. A. Zuttel, A. Borgschulte, L. Schlapbach, *Int. J. Hydrogen Energy*, **27**, 203 (2002).
9. A. E. Y. Marrero, A. M. Beaird, T. A. Davis, M. A. Matthews, *J. Molecular Catalysis*, **48**, 3703 (2009).
10. U. Eberle, M. Felderhoff, *J. German Society*, **48**, 6608 (2009).
11. R. Chahie, T. K. Bose, *J. Hydrogen Energy*, **19**, 161 (1994).
12. A. C. Dillon, K. M. Jones, T. A. Bekkedahl, C. H. Kiang, D. S. Bethune, M. J. Heben, *Applied Physics*, **72**, 133 (2001).
13. S. Hynek W. Fuller Bentley, *Int. J. Hydrogen Energy*, **22**, 601 (1997).
14. M. Kunowsky, B. Weinberger, F. Lamari Darkrim, G. F. Suarez, A. D. Cazorala, L. Solano, *Int. J. Hydrogen Energy*, **33**, 2975 (2008).
15. B. Sakintuna, F. Lamari, *Int. J. Hydrogen Energy*, **32**, 1121 (2007).
16. B. Bogdanovic, M. Schwickardi, *J. Alloys Compounds*, **36**, 302 (2000).
17. V. Diakov, M. Diwan, E. Shaffirovich, A. Varma, *Chem. Eng. Society*, **62**, 5586 (2000).
18. R. B. Binwale, S. Rayalu, S. Devotta, M. Ichikawa, Chemical hydrides, *Int. J. Hydrogen Energy*, **39**, 1390 (2008).
19. Nagar, A. Schechter, B. B. Moshe, N. Shvalb, *Materials and Design*, **108**, 240 (2016).
20. V. Netskina, T. N. Phillipov, O. V. Komova, V. I. Simagina, *Catal. Sustain. Energy*, **41**, (2018).
21. U. B. Demirci, *Turkish J. Chemistry*, **42**, 193 (2018).
22. S. Kaufman, *J. Power Sources*, **85**, 186 (2000).
23. O. Akdim, U. B. Demirci, D. Muller, P. Miele, *Int. J. Hydrogen Energy*, **34**, 2631 (2009).
24. A. Kaur, D. Gangacharyulu, P. K. Bajpai, *Brazilian J. Chem. Eng.*, **35**, 131 (2016).
25. A. Kaur, D. Gangacharyulu, P. K. Bajpai, *Brazilian J. Chem. Eng.*, **36**, 929 (2019).
26. G. F. Froment, K. B. Bischoff, *Chemical Reactor Analysis and Design*, John Wiley and Sons, New York, 1990.
27. J. S. Zhang, W. N. Delgass, T. S. Fisher, J. P. Gore, *J. Power Sources*, **164**, 772 (2007).
28. D. D. Duong, *Adsorption Analysis: Equilibria and Kinetics*, Imperial College Press, London, 1998.
29. D. Mark, J. D. Robert, *Fundamentals of Chemical Reaction Engineering*, McGraw Hill, New York, 2003.
30. M. Mitov, R. Rashkov, N. Atanassov, A. Zielonka, *J. Material Science*, **42**, 3367 (2007).
31. H. B. Dai, Y. Liang, P. Wang, H. M. Cheng, *J. Power Sources*, **177**, 17 (2008).
32. B. H. Liu, Z. P. Li, S. Suda, *J. Alloys and Compounds*, **415**, 288 (2006).
33. L. Soler, A. M. Candela, J. Macanas, M. Munoz, J. Casado, *J. Power Sources*, **192** (2009).
34. G. Sposito, *The Environmental Chemistry of Aluminum*, Lewis Publishers, 1996.
35. J. P. Brunelle, *Pure and Applied Chemistry*, **50**, 1211 (1978).

36. E. Y. M. Alfonso, A. M. Beard, T.A. Davis, M. A. Matthews, *Industrial and Engineering Chemistry Research*, **48**, 3703 (2009).
37. H. Y. Cheng, H. H. Chih, S. T. Chung, *Aerosol and Air Quality Research*, **12**, 745 (2012).
38. H. B. Dai, G. L. Ma, X. D. Kang, P. Wang, *Catalyst Today*, **170**, 50 (2009).

### Supplementary Section

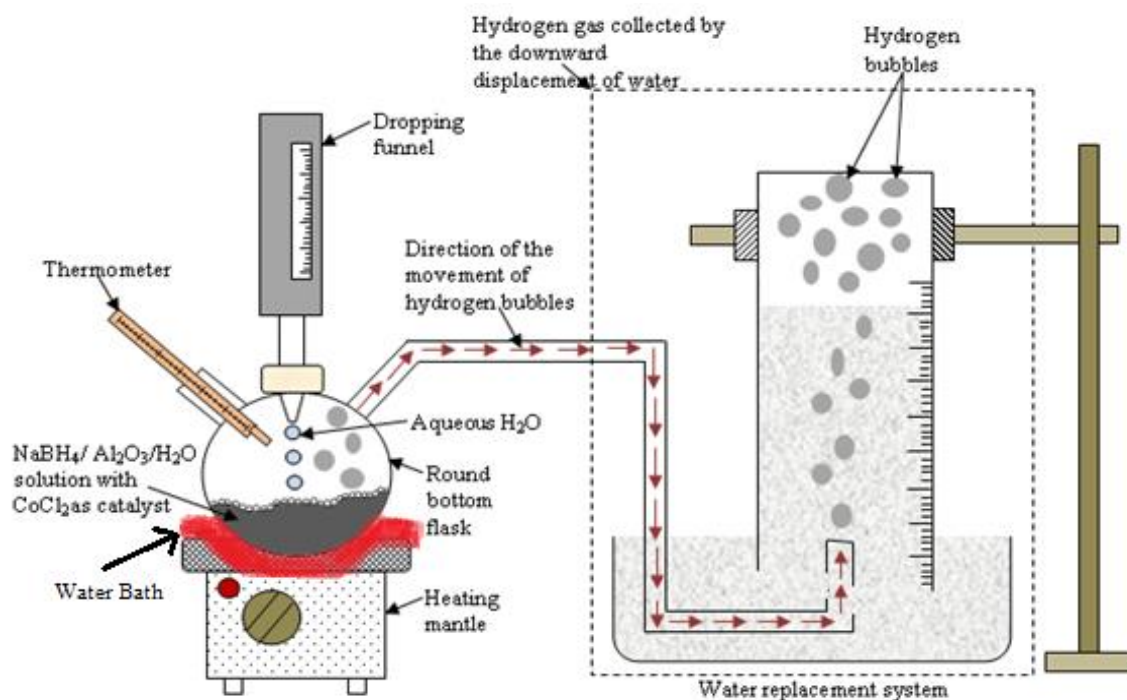


Figure S1. Experimental set up

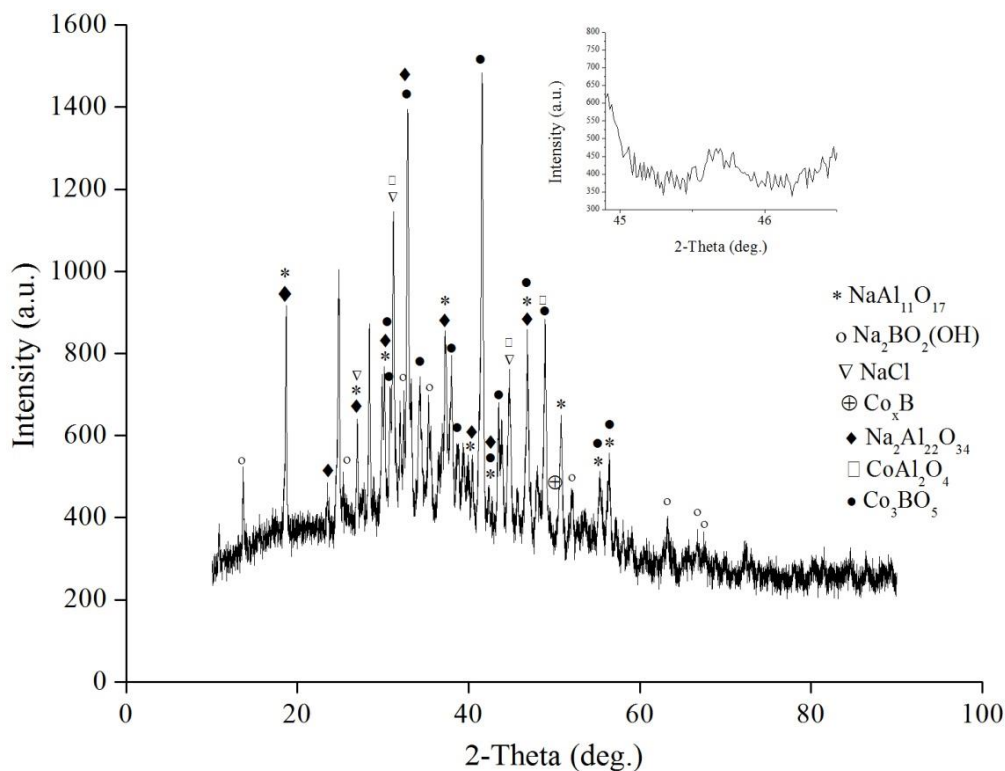
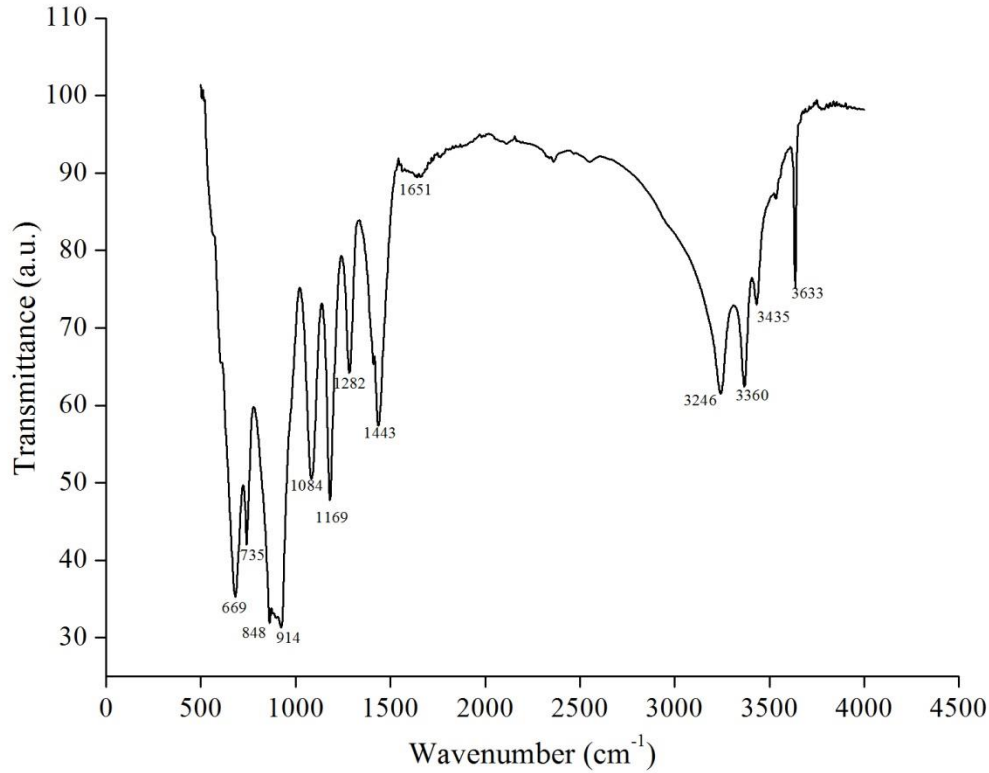


Figure S2. XRD analysis of residue [24]





**Figure S3.** FTIR analysis of residue [24]

Following are the reactions from the literature studies in correspondence with the present system of hydrogen generation.

Active site for chemisorption is given by R with its surface concentration [R]. Adsorption concentration of NaBH<sub>4</sub> is expressed as [C], thus,



Here, [CR] is NaBH<sub>4</sub> that is chemisorbed on the sites of the surface with respect to  $k_{\text{ads}}$  and  $k_{\text{ds}}$  that are rate constants signifying the rate of adsorption and desorption. Hence, the net rate of adsorption is given by [28]:

$$r = k_{\text{ad}}[C][R] - k_{\text{de}}[CR] \quad (S2)$$

Hence, the equilibrium relation becomes,

$$K_{\text{ad}} = \frac{k_{\text{ad}}}{k_{\text{de}}} = \frac{[CR]}{[C][R]} \quad (S3)$$

Also, we introduce [R]<sub>I</sub> that is concentration of all adsorption sites on the catalyst surface and  $\theta_c$  that is the surface coverage of reactants on the catalyst surface.

Therefore,

$$[R]_i = [R] + [CR] \quad (S4)$$

$$\theta_c = \frac{[CR]}{[R]_i} \quad (S5)$$

The fractional surface coverage ( $\theta_c$ ) by the adsorbate borohydride ions could also be obtained from equations S3, S4 and S5 [26]:

$$\theta_c = \frac{[C]K}{1+[C]K} \quad (S7)$$

Here, K is Langmuir adsorption isotherm constant and [C] is concentration of NaBH<sub>4</sub> at time t.

Equations used for calculation of surface coverage of borohydride ions on catalyst surface:

[CR] is written as  $q_e$  in moles/g and [R]<sub>i</sub> is written as  $q_m$  in moles/g for calculation purposes, therefore,

$$\theta_c = \frac{q_e}{q_m} \quad (S8)$$

From equations S7 and S8, the following equation is obtained:

$$\frac{1}{q_e} = \frac{1}{K[C]q_m} + \frac{1}{q_m} \quad (S9)$$

Thus, the plot of  $1/q_e$  and  $1/q_m$  would give the slope and intercept to calculate  $k_{\text{ad}}$  and  $q_m$  [4].